The Photon Content of the Unpolarized and Polarized Nucleon *

Asmita Mukherjee
(Universität Dortmund)

- Equivalent photon approximation (EPA)
- QED Compton process : (i) extract EPA
  (ii) measure $F_{1,2}$ and $g_{1,2}$
- QED Compton process at HERMES
- QED Compton process at eRHIC
  comparison with HERMES
- Suppression of background virtual Compton scattering (VCS)
- Summary and conclusion

* In collaboration with M. Glück, C. Pisano, E. Reya
(Dortmund)

Equivalent Photon Approximation (EPA)

- Based on the Equivalent Photon Approximation of a pointlike charged fermion.
- The EPA can be extended to the nucleon $N = p, n$ (non-pointlike particle) as an efficient tool to estimate high energy cross sections :

$$(\Delta)\sigma_{NX} \approx (\Delta)\sigma_{NX}^{\mathrm{EPA}} = (\Delta)\gamma \otimes (\Delta)\hat{\sigma}_{\gamma X}$$

- In $(\Delta)\sigma_{NX}$

  $X = l, N$ interacts with N via virtual photon
  $Q^2 = -t = -k^2$: virtuality of the photon

  The EPA is a good approx. when Q^2 is small

- In $(\Delta)\sigma_{NX}^{\mathrm{EPA}}$
  $(\Delta)\hat{\sigma}_{\gamma X}$: real photoproduction cross section

  μ^2: momentum scale in $(\Delta)\hat{\sigma}_{\gamma X}$

  x: fraction of the proton's momentum carried by the (collinear) photon

- $(\Delta)\gamma(x, \mu^2)$: universal, scale dependent, equivalent photon distribution of the nucleon

$$(\Delta)\gamma(x, \mu^2) = (\Delta)\gamma_{el}(x) + (\Delta)\gamma_{inel}(x, \mu^2)$$

- The kinematical region of validity of $(\Delta)\gamma(x, \mu^2)$ has to be tested
- Has a different evolution compared to $(\Delta)g(x, \mu^2)$.

- In terms of the elastic form factors $G_E(t)$, $G_M(t)$ (m: nucleon mass, $\tau = -t/4m^2$):

$$\Delta\gamma_{e\ell}(x) = -\frac{\alpha}{2\pi}\int_{t_{\min}}^{t_{\max}} \frac{dt}{t}\left\{\left[2 - x + \frac{2m^2x^2}{t}\right] G_M^2(t) \right.$$
$$\left. -2\left[1 - x + \frac{m^2x^2}{t}\right] G_M(t)\frac{G_M(t) - G_E(t)}{1+\tau}\right\}$$

Glück, Pisano, Reya

$$\gamma_{e\ell}(x) = -\frac{\alpha}{2\pi}x\int_{t_{\min}}^{t_{\max}} \frac{dt}{t}\left\{2\left[\frac{1}{x}\left(\frac{1}{x} - 1\right) + \frac{m^2}{t}\right]\right.$$
$$\left. \times \frac{G_E^2(t) + \tau G_M^2(t)}{1+\tau} + G_M^2(t)\right\}$$

Kniehl

$t_{\min} \approx -\infty$, $t_{\max} \approx -m^2x^2/(1-x)$

$\rightsquigarrow$ $(\Delta)\gamma_{e\ell}(x)$ can be integrated analytically

- The inelastic part $(\Delta)\gamma_{ine\ell}$ obeys the LO evolution equation

$$\frac{d}{d\ln\mu^2}(\Delta)\gamma_{ine\ell}(x,\mu^2) = \frac{\alpha}{2\pi}\sum_{q=u,d,s} e_q^2 \int_x^1 \frac{dy}{y}$$
$$\times (\Delta)P_{\gamma q}\left(\frac{x}{y}\right)\left[(\Delta)q(y,\mu^2) + (\Delta)\bar{q}(y,\mu^2)\right]$$

Glück, Stratmann, Vogelsang; Glück, Pisano, Reya

$\Delta P_{\gamma q}(y) = 2 - y$, $P_{\gamma q}(y) = [1 + (1-y)^2]/y$

$\Delta\overset{(-)}{q}$: LO pol. parton distr. GRSV2001 (v.s.)

$\overset{(-)}{q}$: LO unpol. parton distr. GRV98

'minimal' not compelling boundary condition $(\Delta)\gamma_{ine\ell} = 0$ at $\mu_0^2 = 0.26$ GeV^2

Photon distribution of the proton

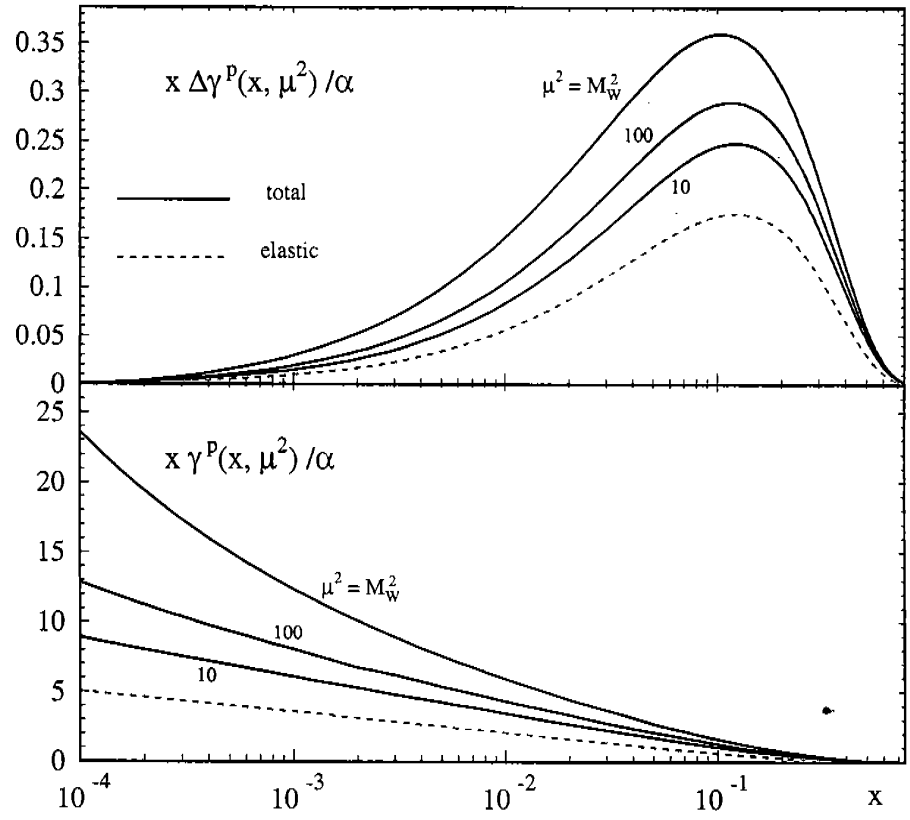

μ^2 is in GeV^2

$x\,\Delta\gamma^p(x,\mu^2)$ vanishes at small x, $x\,\gamma^p(x,\mu^2)$ increases:

$\Delta\gamma^p(x,\mu^2) \ll \gamma^p(x,\mu^2)$, for $x \leq 10^{-3}$

$x\,\Delta\gamma^p_{e\ell}(x),\ x\,\Delta\gamma^p_{ine\ell}(x,\mu^2) \to 0$ as $x \to 0$

$x\,\gamma^p_{e\ell}(x),\ x\,\gamma^p_{ine\ell}(x,\mu^2) \to \infty$ as $x \to 0$

$\Delta\gamma^p_{e\ell}(x)/\gamma^p_{e\ell}(x) \to 1$ as $x \to 1$

- The elastic contribution dominates at moderate values of μ^2:
  $(\Delta)\gamma^p_{e\ell}(x) \geq (\Delta)\gamma^p_{ine\ell}(x,\mu^2)$, for $\mu^2 \leq 100\,\text{GeV}^2$

Glück, Pisano, Reya

Photon distribution of the neutron

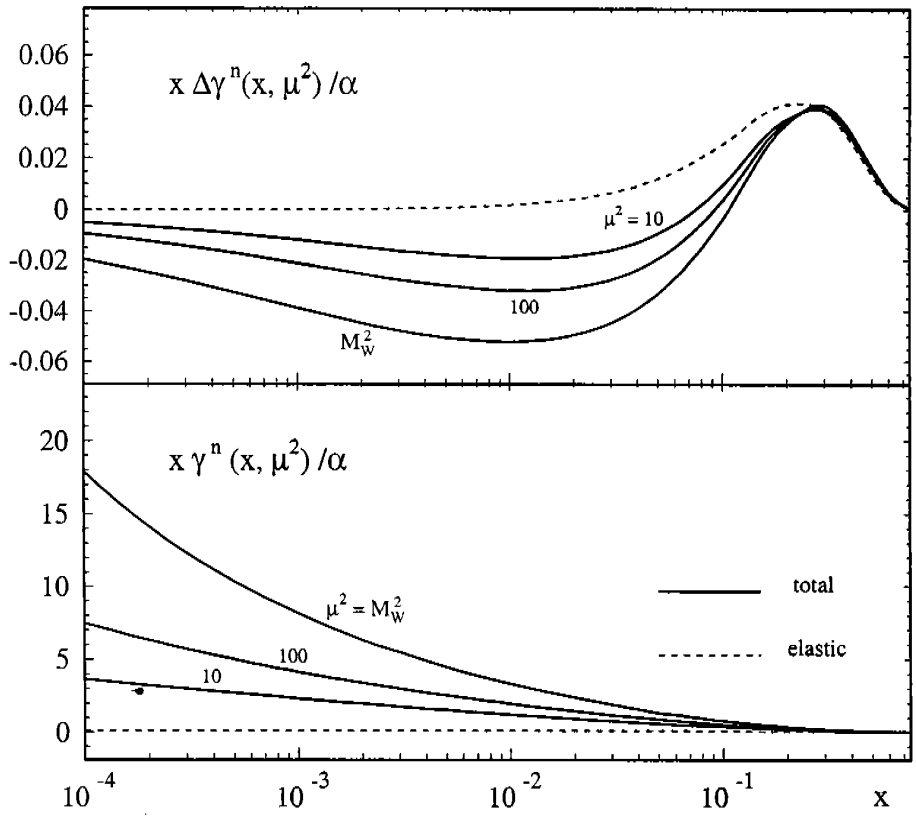

$\Delta\gamma^n(x,\mu^2)$ is sizeable smaller than $\Delta\gamma^p(x,\mu^2)$

$\Delta\gamma^n_{inel}(x,\mu^2)$ is marginal for $x \geq 0.2$,

$\gamma^n_{el}(x)$ is marginal and non-singular as $x \to 0$

At small x, $(\Delta)\gamma^n(x,\mu^2)$ behaves as $(\Delta)\gamma^p(x,\mu^2)$:

$x\,\Delta\gamma^n_{el}(x)$, $x\,\Delta\gamma^n_{inel}(x,\mu^2) \to 0$ as $x \to 0$

$x\,\gamma^n_{el}(x) \to 0.078$, $x\,\gamma^n_{inel}(x,\mu^2) \to \infty$ as $x \to 0$

$\Delta\gamma^n_{el}(x)/\gamma^n_{el}(x) \to 6/7$ as $x \to 1$

Glück, Pisano, Reya

QED Compton Scattering

$$e(l) + p(P) \rightarrow e(l') + \gamma(k') + X(P_X),$$

X is a proton with momentum P' for elastic scattering.

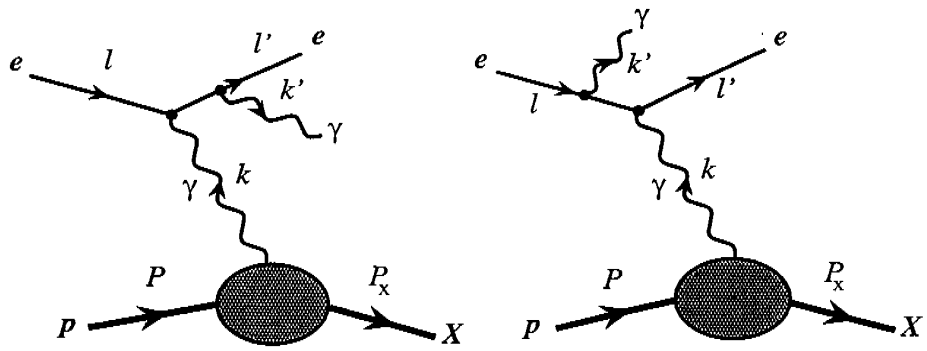

• Virtual Compton Scattering → photon radiated from the proton : background

• Cross section has several peaks :

Outgoing photon is emitted along the incident electron line (ISR).

Outgoing photon is emitted along the final electron line (FSR).

• QED Compton Peak : $Q^2 = -k^2 \approx 0$ but the electron propagators are not too small

Distinctive experimental signature: outgoing electron and photon are detected at large polar angles and almost back-to-back in azymuth, with little or no hadronic activity at the detectors.

• QED Compton events are singled out by imposing a cut on the total transverse momentum of the $e - \gamma$ system or, on the acoplanarity

$$A = 180° - \mid \Delta\phi \mid,$$

where $\Delta\phi$ is the angle between the transverse momenta $\vec{p}_{t,e}$ and $\vec{p}_{t,\gamma}$.

• QED Compton peak in unpol. $e-p$ scattering : measurement of $F_2(x_B, Q^2)$

Courau, Kessler; Blümlein, Levman, Spiesberger; Lendermann, Schultz-Coulon, Wegener : low-Q^2, medium x_B (not well known from other experiments)

• QED corrections to polarized DIS :
Bardin, Blümlein, Christova, Kalinovskaya

• Fixed target experiments : F_2 and g_1 at low Q^2 and low x_B;
CLAS : $Q^2 = 0.15 - 1.6\ GeV^2$.

• Polarized $e-p$ collider: broader range of x_B and Q^2 $\rightarrow$ measurement of g_1 by measuring the QED Compton peak.

• Determination of g_1 at lower Q^2 region is important to test various models $\rightarrow$ nonperturbative effects $\rightarrow$ resonance contributions, higher twist; resummation effects at low x_B

Also important is the transition region from from soft to hard physics.

• Another interesting aspect : Extraction of the equivalent photon distribution of the polarized proton and to find the kinematical region of validity of the equivalent photon approximation.

unpol. Courau, Kessler; Blümlein, Levman, Spiesberger; Rujula, Vogelsang; AM, Pisano; pol. Glück, Pisano, Reya, Schienbein; AM, Pisano

QED Compton Process in the EPA

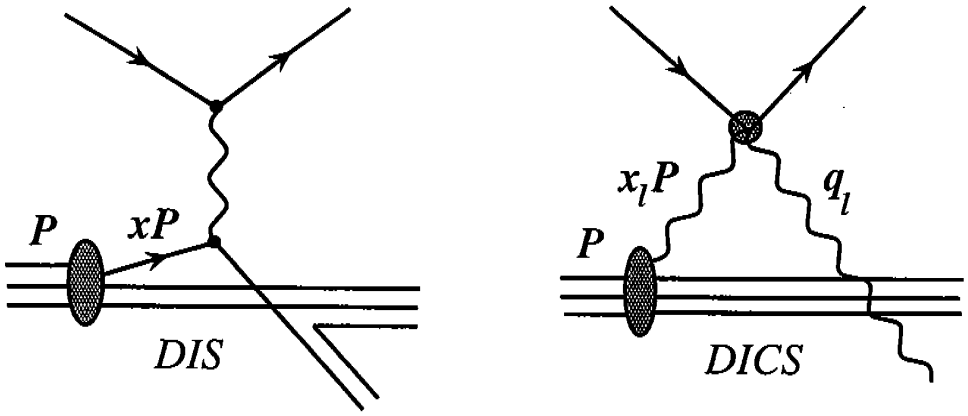

- Probing the photon in the proton by a lepton
- Event kinematics is constrained by two variables like inclusive ep scattering.

Define $Q_l^2 = -\hat{t} = -(l - l')^2$; $\quad x_l = \frac{Q_l^2}{2P.(l-l')}$

$$\frac{d^2(\Delta)\sigma}{dx_l dQ_l^2} = \int_0^1 \frac{dz}{z}(\Delta)\gamma(z, Q_l^2)\frac{d^2(\Delta)\hat{\sigma}^{e\gamma\to e\gamma}}{d(\frac{x_l}{z})dQ_l^2}.$$

$$\gamma_{\text{inel}}(x, xS) = \frac{\alpha}{2\pi}\int_x^1 dy \int_{Q^2_{\text{min}}}^{Q^2_{\text{max}}} \frac{dQ^2}{Q^2}\frac{y}{x}\left[F_2\left(\frac{x}{y}, Q^2\right)\left(\frac{1+(1-y)^2}{y^2} - \frac{2m^2x^2}{y^2Q^2}\right) - F_L\left(\frac{x}{y}, Q^2\right)\right].$$

$$\Delta\gamma_{\text{inel}}(x, xS) = \frac{\alpha}{2\pi}\int_x^1 \frac{dy}{y}\int_{Q^2_{\text{min}}}^{Q^2_{\text{max}}} \frac{dQ^2}{Q^2}\left(2 - y - \frac{2m^2x^2}{Q^2}\right)2g_1(\frac{x}{y}, Q^2),$$

$Q^2_{\text{min}} = \frac{x^2m^2}{1-x}$, $\qquad Q^2_{\text{max}} = \hat{s}$

$\hat{s} = (l' + k')^2, S = (l + P)^2, \qquad x = \frac{\hat{s}}{S};\ S >> m^2,\ \hat{s} >> Q^2$

QED Compton process at HERMES

- The 'exact' $(\Delta)\sigma$ compared with the EPA; EPA expressed in terms of structure functions

AM, Pisano

- $(\Delta)\sigma$ and $(\Delta)\sigma^{\mathrm{EPA}}$ are in x_γ bins, $x_\gamma = \frac{l\cdot k}{P\cdot l}$

x_γ : fraction of longitudinal momentum of the proton carried by the photon

- Bins in $x_l = \frac{-\hat{t}}{2P\cdot(l-l')}$ can also be used

$\rightsquigarrow$ $x_\gamma \simeq x_l \simeq x = \frac{\hat{s}}{S}$ as $Q^2 \simeq 0$; $\hat{s} = (l'+k')^2, S = (l+P)^2$

- F_2 param. ALLM97 (Also valid at low-Q^2) ; Callan-Gross reln. $E_e = 27.5$ GeV

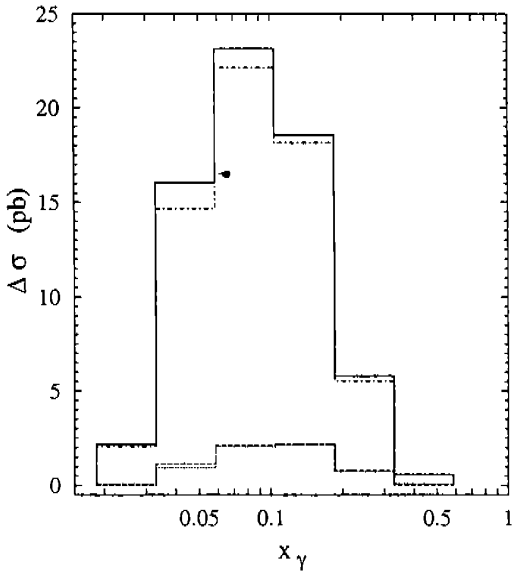

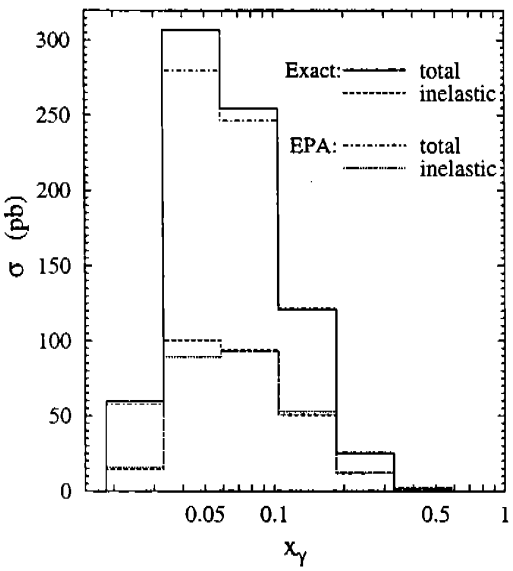

$g_2 \approx 0$, g_1: Badelek, Kwiecinski, Ziaja.

- Kinematical cuts: $E'_e, E'_\gamma > 4\,\mathrm{GeV}$, $\hat{s} > 1\,\mathrm{GeV}^2$, $0.04 < \theta_e, \theta_\gamma < 0.2$, $\hat{s} > Q^2$

Suppress the radiative events unrelated to QED Compton scattering

Major background from VCS is suppressed by the exp. condition of no observable hadronic activity at the detectors.

QED Compton process at HERMES (II)

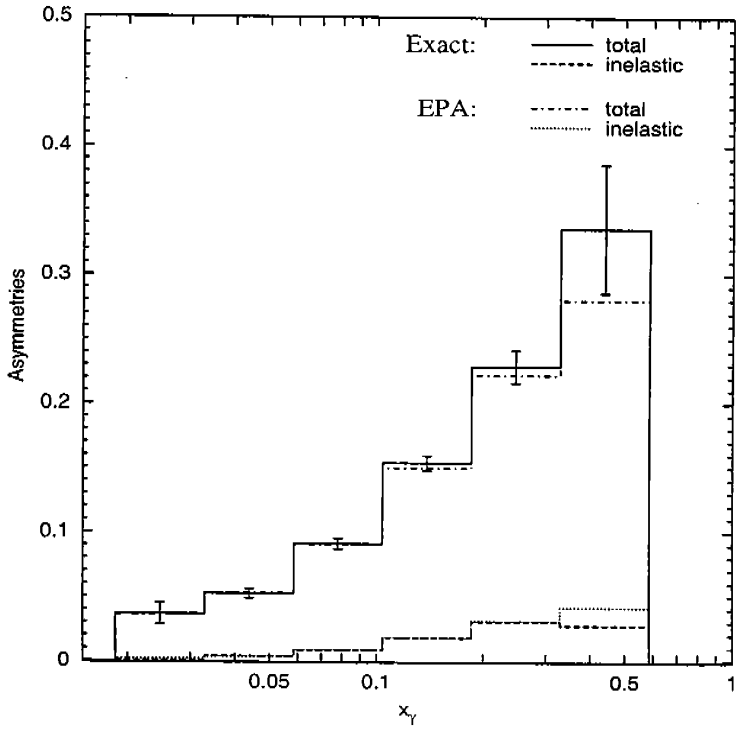

- Asymmetry $A_{LL} = \frac{d\Delta\sigma}{d\sigma}$

$\Delta\sigma = \frac{1}{2}(\sigma_{++} - \sigma_{+-})$; $\quad \sigma = \frac{1}{2}(\sigma_{++} + \sigma_{+-})$

- Discrepancy of 'exact' with the EPA small for small to medium x_γ
- Expected statistical error increases in higher x_γ bins:

Error: $\delta A_{LL} \approx \frac{1}{P_e P_p \sqrt{\mathcal{L}\sigma_{bin}}}$; $P_e = P_p = 0.7$, $\mathcal{L} = 1/fb$.

$\frac{\Delta\sigma^{\mathrm{EPA}} - \Delta\sigma}{\Delta\sigma} = -4.8\%$, $\qquad \frac{\sigma^{\mathrm{EPA}} - \sigma}{\sigma} = -4.7\%$

$\frac{\Delta\sigma_{e\ell}^{\mathrm{EPA}} - \Delta\sigma_{e\ell}}{\Delta\sigma_{e\ell}} = -5.0\%$, $\qquad \frac{\sigma_{e\ell}^{\mathrm{EPA}} - \sigma_{e\ell}}{\sigma_{e\ell}} = -5.7\%$

- $g_1(x_B, Q^2)$ Measurement at HERMES using QED Compton peak : events can be observed

x_B : $0.02 - 0.5$
Q^2 : $0.007 - 7 \;\; GeV^2$

(subject to the constraints discussed before)

QED Compton process at eRHIC

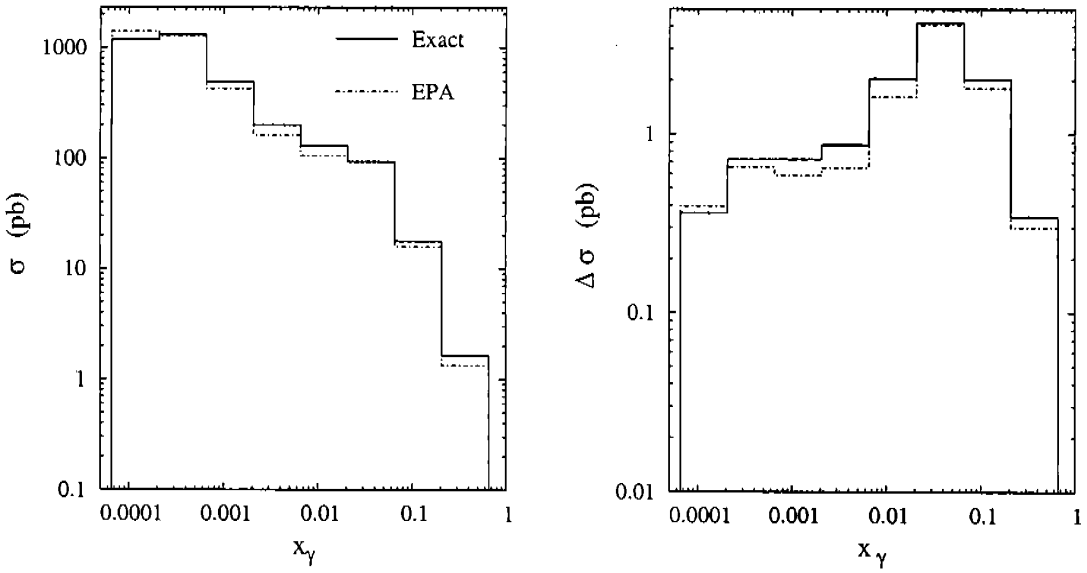

- $(\Delta)\sigma$ and $(\Delta)\sigma^{\mathrm{EPA}}$ are in x_γ bins, $x_\gamma = \frac{l\cdot k}{P\cdot l}$

- $E_e = 10$ GeV, $E_p = 250$ GeV

- Kinematical region :

$E'_e, E'_\gamma > 4\ GeV; \quad \hat{s} > 1\ \ GeV^2$
$0.06 \leq \theta_e, \theta_\gamma \leq \pi - 0.06$
$\hat{s} > Q^2$

- F_2 param. ALLM97 (Also valid at low-Q^2) ; Callan-Gross reln.

$g_2 \approx 0$, g_1: Badelek, Kwiecinski, Ziaja.

- $\frac{\Delta\sigma^{\mathrm{EPA}} - \Delta\sigma}{\Delta\sigma} = -9.8\%, \qquad \frac{\sigma^{\mathrm{EPA}} - \sigma}{\sigma} = 1.2\%$

QED Compton Process at eRHIC (II)

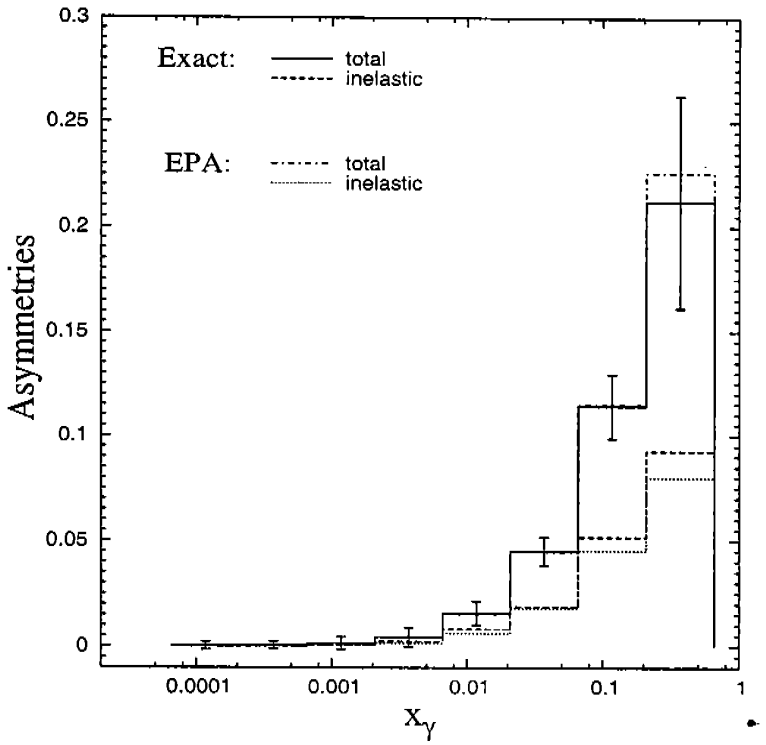

- Asymmetry very small for smaller x_γ bins; increases as x_γ increases

- Agreement with the EPA better except in the last bin

- Expected statistical error is large for high x_γ bins:

Error: $\delta A_{LL} \approx \frac{1}{P_e P_p \sqrt{\mathcal{L}\sigma_{bin}}}$; $P_e = P_p = 0.7$, $\mathcal{L} = 1/fb$.

- g_1 measurement at eRHIC using QED Compton peak :

Broader x_B, Q^2 range subject to the kinematical cuts shown before

x_B : 1×10^{-4} and above
Q^2 : $.003 - 1000 \quad GeV^2$

Suitable to test models of g_1 at low-Q^2 as well as in the transition region

Virtual Compton Scattering Background

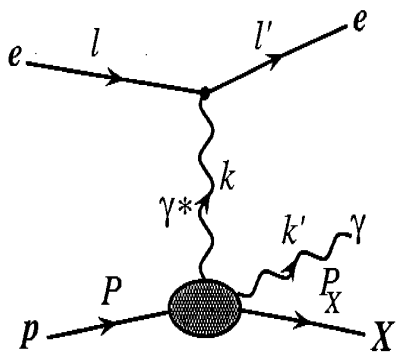

Elastic contribution : in terms of generalized parton distributions. Monte Carlo estimate for HERA : suppressed

To estimate the inelastic contribution, convolute cross section of subprocess

$$e(l) + q(p) \to e(l') + \gamma(k') + q(p'),$$

with an 'effective' parton distribution of the proton:

$$\tilde{q}(x_B, Q^2) = \frac{Q^2}{Q^2 + a\,Q_0^2}\, q(x_B, Q^2 + Q_0^2),$$

Parameters : $a = 1/4$ and $Q_0^2 = 0.4\,\mathrm{GeV}^2$, $q(x_B, Q^2)$: NLO GRV98.

Polarized : convolute with the effective polarized distribution

$$\Delta\tilde{q}(x_B, Q^2) = \Delta q(\bar{x}, Q^2 + Q_0^2),$$

with $\bar{x} = \frac{x_B(Q^2+Q_0^2)}{(Q^2+x_B Q_0^2)}$; $Q_0^2 = 2.3\ \ GeV^2$; NLO GRSV00 s.s.

Suppression of VCS Background (eRHIC)

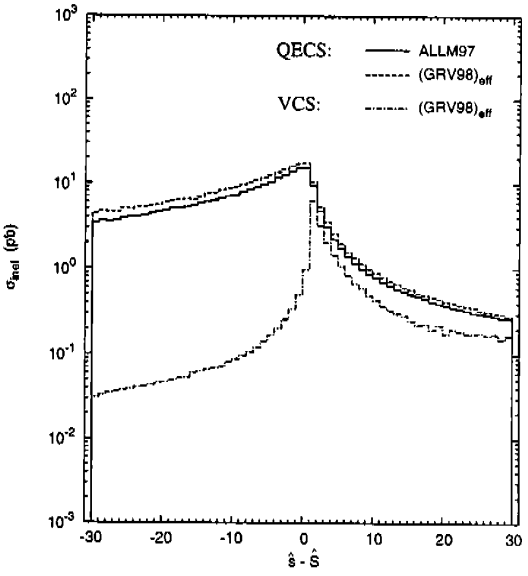

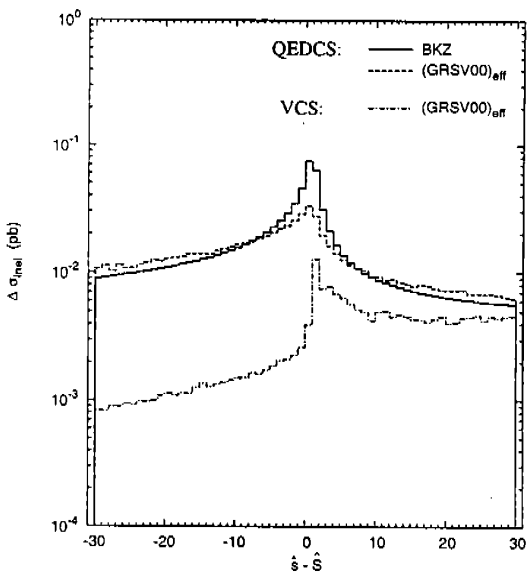

- Integrated cross section:

$$\sigma_{\text{inel}}(S) = \sum_q \int \frac{dx_B}{x_B^2} \int d\hat{s} \int dQ^2 \int d\hat{t} \int d\varphi^* \frac{1}{(\hat{s}+Q^2)} \overline{|M_{inel}|^2} \tilde{q}(x_B, Q^2)$$

$$\overline{|M_{inel}|^2} = \overline{|M_{inel}^{QEDCS}|^2} + \overline{|M_{inel}^{VCS}|^2} - 2\,\Re e \overline{M_{inel}^{QEDCS} M_{inel}^{VCS*}}.$$

- 'Effective' parton model estimate of VCS background
- Invariants : $\hat{S} = (p'+k')^2 = \frac{\hat{t}(x_l - x_B)}{x_l}$;

with $\hat{t} = (l-l')^2$, $x_l = \frac{-\hat{t}}{2P\cdot(l-l')}$ and $\hat{s} = (l'+k')^2$.

- Inelastic interference between QEDCS and VCS: negligible.
- VCS is suppressed when $\hat{s} < \hat{S}$.

Summary and Conclusion

- The photon content of polarized and unpolarized nucleon $(\Delta)\gamma^N(x,\mu^2)$
evaluated in the EPA gives an estimate of the photon-induced subprocesses in elastic/deep inelastic eN and hadronic $(pN,...)$ reactions.

- Polarized : Can be extracted experimentally at HERMES/eRHIC: through QED Compton process in $ep \to e\gamma p$ and $ep \to e\gamma X$: distinctive experimental signature.

- Unpolarized : at HERA

- QED Compton peak in polarized ep scattering : Will provide informations concerning the structure functions $g_{1,2}$ in the low Q^2 region at HERMES; future polarized ep collider: over a broad range of x_B, Q^2 .

- Discussed relevant kinematical cuts in order to select QEDC events from experiments; both for fixed target (HERMES) and collider (eRHIC) kinematics.